

are shorted. It operates in the fundamental mode $TE_{0,5,0}$ [8]. The radiating U-slot is etched in the top wall of the HMSIW at the distance L_{viaX} from its short end in the x-direction, and from the row of vias at the distance W_{viaY} in the y-direction. The outer dimensions of the slot are $L_{\text{SLOT-X}}$ and $L_{\text{SLOT-Y}}$. The width of the slot is W_{SLOT} . The slot is shorted by the strip of the length L_{SHORT} . The shorting via is placed between the area bounded by the slot and the HMSIW bottom wall at the distances X_{VIA} and Y_{VIA} from the slot edges in the x- and y-direction, respectively. The antenna is equipped by a HMSIW-to-SMA transition.

The antenna radiates a left-handed circularly polarized wave in the boresight direction. The right-handed circularly polarized wave can be obtained by mirroring the antenna with respect to the x-z plane.

3. Antenna Design and Experimental Verification of the Antenna

The antenna design procedure can be divided into the following steps:

1. Design of the HMSIW using (8) – (13) presented in [8]. The waveguide should operate in the fundamental mode $TE_{0,5,0}$. The operating frequency of the antenna should be approximately 1.5 times higher than the cut-off frequency of the fundamental mode.

2. Preliminary determination of the slot dimensions. The lengths $L_{\text{SLOT-X}}$ and $L_{\text{SLOT-Y}}$ of the slot should be lesser than λ_m and a half of λ_m in the x- and in y-direction, respectively. (λ_m is the wavelength in the dielectric substrate at the design frequency). The best initial lengths $L_{\text{SLOT-X}}$ and $L_{\text{SLOT-Y}}$ of the slot should be approximately $0.75 \lambda_m$ and $0.4 \lambda_m$ in the x- and in y-direction, respectively. The width of the slot W_{SLOT} should be only several hundredths of λ_m , e.g. $\lambda_m/20$. The shorting via I_1 should be placed in the right half of the area bounded by the slot. The best placing of shorting via I_1 for further optimization is in the distance $X_{\text{via}} \sim 0.15 \lambda_m$ and $Y_{\text{via}} \sim \lambda_m/5$ from the edge of the slot. The slot should be placed in the distance $\lambda_m/4$ from the coaxial probe.

3. Determination of the coax probe position. The coax probe should be placed in the distance approximately $\lambda_m/4$ from the shorted end of the HMSIW in the x-direction and as much as close the magnetic wall of HMSIW in the y-direction.

4. Application of the optimization process. In order to tune the antenna for desired operating frequency band, the optimization procedure with the combination of a full wave solver has to be applied.

The proposed antenna is designed with the help of time domain solver of CST Microwave Studio (CST MWS), where local optimizations Trust Region Framework and Nedler Mead Simplex Algorithm were used for the operating frequency of 10 GHz on the dielectric substrate ARLON Cuclad 217 with the relative permittivity $\epsilon_r = 2.17 \pm 0.02$, tangent loss $\tan(\delta) = 0.0009$, and height $h =$

	[mm]		[mm]
L	37.5	Y_{COAX}	0.8
$L_{\text{SLOT-X}}$	14.6	X_{VIA}	3.25
$L_{\text{SLOT-Y}}$	7.2	Y_{VIA}	2.65
L_{viaX}	2.8	G_{viaX1}	4.2
W	18.0	G_{viaX2}	7.5
W_{HMSIW}	8.9	G_{viaY}	6.1
W_{SHORT}	0.3	H	1.524
L_{viaY}	1.7	d_{11}	1.4
W_{SLOT}	1.1	D	1.4
W_{AP}	3.0	P	2.58
X_{COAX}	3.0		

Tab. 1. Dimensions of the proposed antenna (Fig. 1).

1.524 mm. The resultant dimensions of the antenna are summarized in Tab. 1.

The distribution of the electric field in the substrate at the frequency 10 GHz is depicted in Fig. 2. Thanks to the shorting via I_1 , the electric field at the slot rotates and the left handed circularly polarized wave in the far field is obtained. Simulated 3D radiation patterns for LHCP and RHCP at operating frequency 10 GHz are depicted in Fig. 3. The simulated realized gain is 5.99 dBi for LHCP.

To verify the proposed antenna concept (Fig. 1) experimentally, the antenna was fabricated (Fig. 4) by a low-cost etching PCB process with estimated precision of about tens of micrometers and drilled with Bungard CCD/ATC (Computer Controlled Drilling machine with Automatic Tool Change) with position accuracy of 20 ppm. The diameter of the tool which was used for drilling is 1.4 mm. The reflection coefficient was measured in a laboratory environment, the radiation patterns for the Theta range from -90° to 90° and the axial ratio were measured in an anechoic chamber. For the measurement, Rohde&Schwarz vector network analyzer ZVA67 was used. The results of the measurement are depicted and compared with the results from CST Microwave Studio in Figs. 5–7.

The simulated and measured reflection coefficient of the antenna is depicted in Fig. 5. The measured results are about 110 MHz shifted to higher frequencies in comparison to the simulated ones due to the manufacturing tolerance. The measured impedance bandwidth of the fabricated sample of the antenna is 11.9% (for $S_{11} < -10$ dB).

The simulated and measured axial ratio at the boresight direction (z-axis direction) versus frequency is plotted in Fig. 6. The measured results are shifted about 80 MHz to higher frequencies in comparison to the simulated ones. The measured axial ratio bandwidth is 2.2% (for $AR < 3$ dB).

The normalized simulated and measured radiation patterns in two orthogonal cutting planes at the frequency 10 GHz are depicted in Fig. 7. In the xz-plane, it can be observed that the radiation pattern is shifted about 8° in comparison to the simulated results. In the yz-plane, the simulated and measured values are in good agreement. The measured peak gain of the antenna is 6.0 dBi.

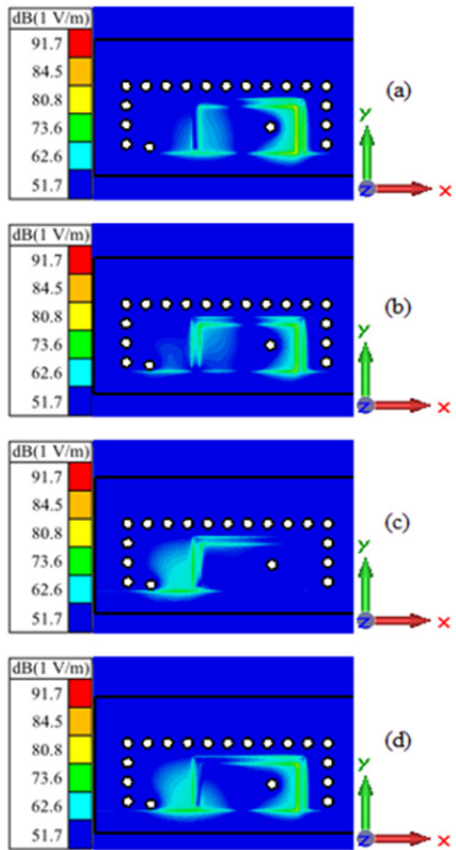


Fig. 2. Distribution of electric field intensity at 10 GHz in substrate (magnitude): (a) phase = 0°, (b) phase = 45°, (c) phase = 90° and (d) phase = 135°.

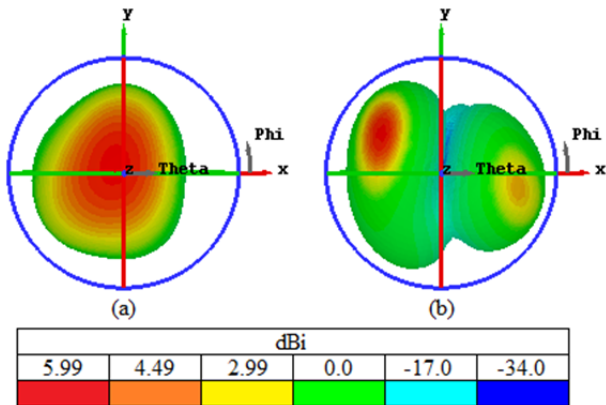


Fig. 3. Simulated radiation patterns of the proposed antenna (realized gain, $f=10$ GHz): (a) LHCP and (b) RHCP.

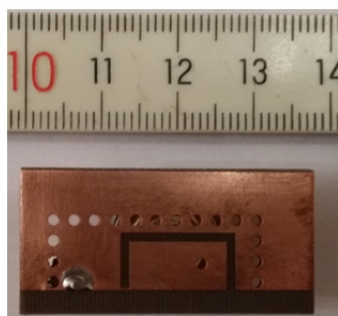


Fig. 4. Fabricated sample of the proposed HMSIW U-slot antenna.

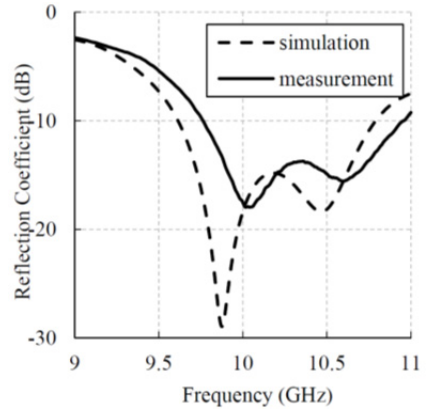


Fig. 5. Reflection coefficient of the proposed antenna.

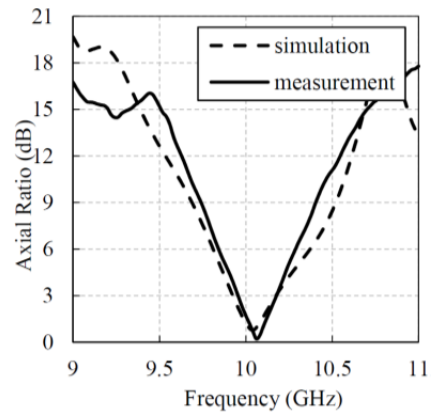


Fig. 6. Axial ratio of the proposed antenna.

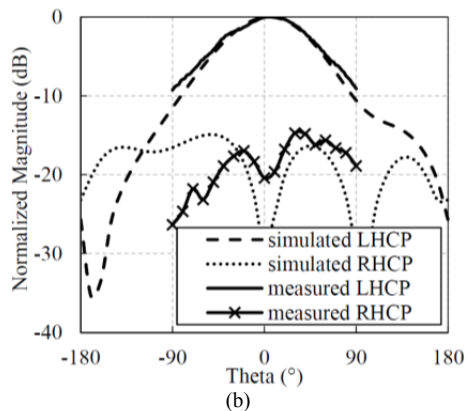
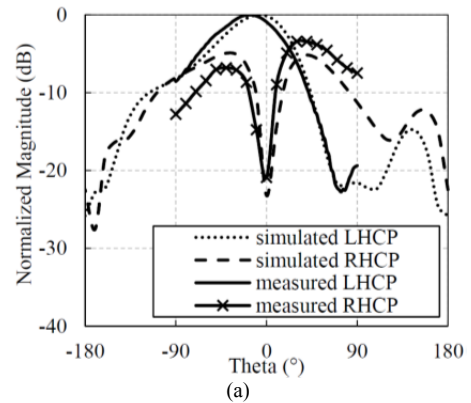


Fig. 7. Normalized radiation patterns of the proposed antenna: (a) xz-plane, (b) yz-plane.

Comparison of circularly polarized single layer HMSIW antennas is summarized in Tab. 2. Obviously, the proposed HMSIW antenna has a lower gain than SIW antenna presented in [6] ($BW = 10.3\%$, $G = 8.0$ dBi and $AR = 2.6\%$), but the size is reduced about 50%. Other parameters are almost the same. The proposed antenna has a wider impedance and axial ratio bandwidth than the antennas presented in [9] and [10]. The proposed antenna is smaller in comparison to other HMSIW antennas.

	impedance BW [%]	gain [dBi]	axial ratio BW [%]	size of antenna
Antenna with dielectric aperture [9]	6.0	4.2	0.7	$0.73 \lambda_0$ $\times 0.22 \lambda_0$
Hybrid antenna [10]	10.0	6.8	1.0	$1.45 \lambda_0$ $\times 1.45 \lambda_0$
Proposed antenna	11.9	6.0	2.2	$0.64 \lambda_0$ $\times 0.24 \lambda_0$

Tab. 2. Comparison of circularly polarized single layer HMSIW antennas (where λ_0 is wavelength in vacuum).

4. Parametric Study

To better understand antenna behavior, the parametric study of the antenna is carried out with help of CST MWS

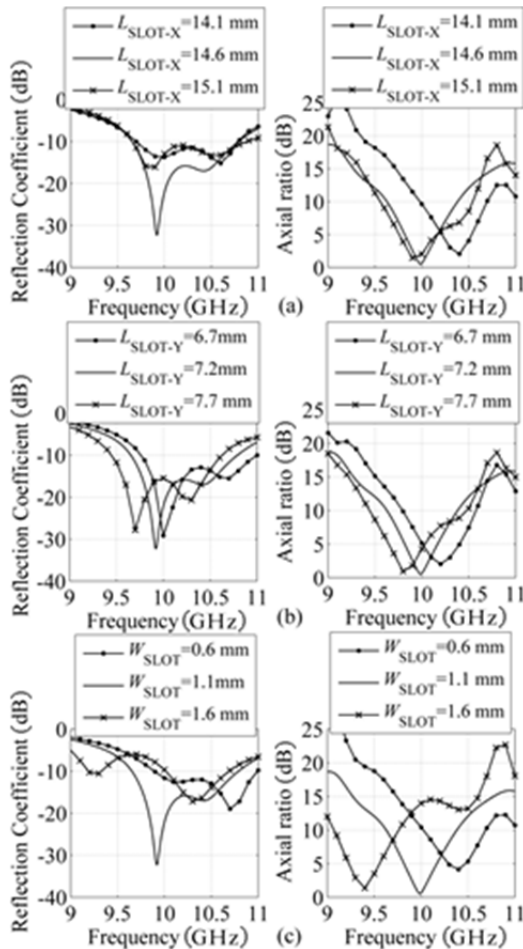


Fig. 8. The effect of the selected parameters on the reflection coefficient and the axial ratio of the proposed antenna: (a) length of slot L_{SLOT-X} in x-direction, (b) length of slot L_{SLOT-Y} in y-direction and (c) width of slot W_{SLOT} .

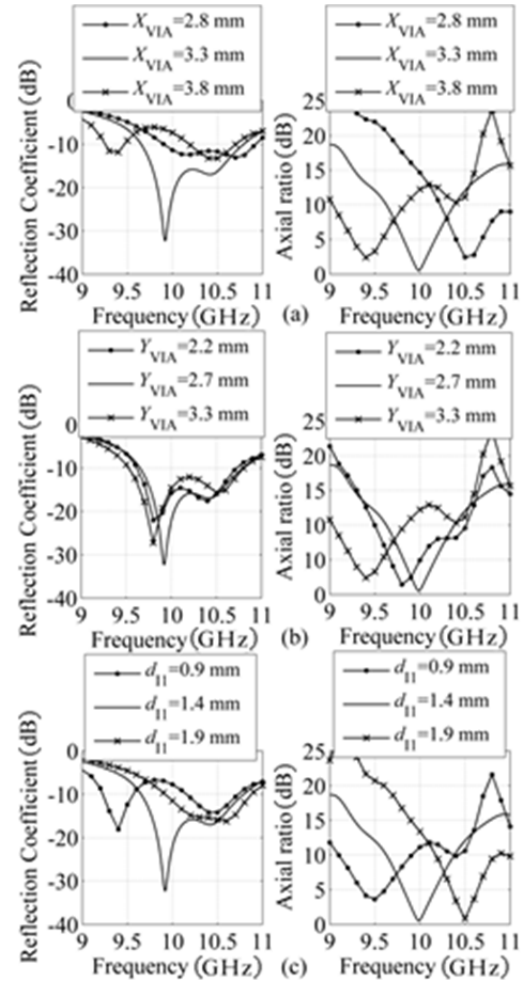


Fig. 9. The effect of the selected parameters on the reflection coefficient and the axial ratio of the proposed antenna: (a) distance X_{VIA} between the slot and the shorting via in x-direction, (b) distance Y_{VIA} between the slot and the shorting via I_1 in y-direction and (c) diameter of the shorting via I_1 .

to demonstrate the effect of antenna geometrical parameters on the reflection coefficient and axial ratio. During this study all parameters given in Tab. 1 are kept and only one parameter is changed. The results are depicted in Fig. 8.

Figures 8(a) and 8(b) show the effect of varying the length of the slot in the x and y direction on the reflection coefficient and the axial ratio of the antenna. Decreasing the slot length L_{SLOT-X} (the x-direction) leads to the deterioration of the impedance matching and shift of the minimum of the axial ratio towards higher frequencies. Decreasing the slot length L_{SLOT-Y} leads to the shift of the operating frequency and the minimum of the axial ratio towards higher frequencies. Figure 8(c) shows the effect of varying the width of the slot W_{SLOT} . The change of the width of the slot has very strong effect on the impedance matching and the axial ratio of the antenna.

Figures 9(a) and 9(b) show the effect of varying the position of the shorting via in the x-direction and y-direction. Obviously, the change of the shorting via position in the x-direction (variation of the parameter X_{VIA}) has much stronger influence on the operating frequency and axial

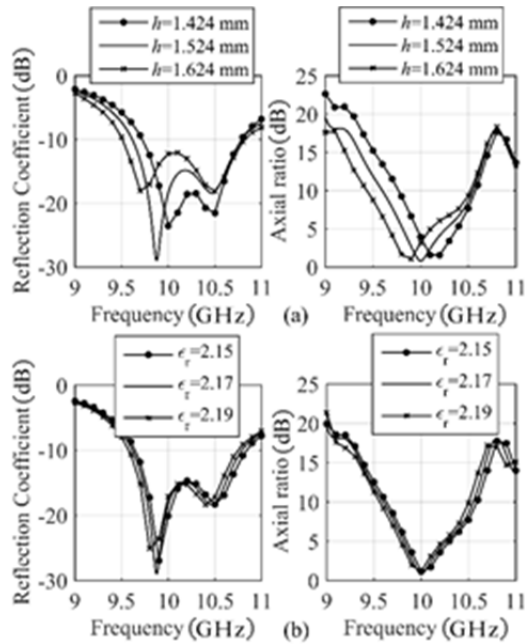


Fig. 10. The effect of the selected parameters of the substrate on the reflection coefficient and the axial ratio of the proposed antenna: (a) height h of the substrate and (b) dielectric constant ϵ_r of the substrate.

ratio than the variation of the in the y-direction (variation of the parameter Y_{VIA}).

Figure 9(c) shows the effect of varying the diameter of the shorting via I_1 . The diameter of the shorting via I_1 influences the operating frequency and the minimum of the axial ratio. Decreasing the diameter of I_1 leads to the shift of the operating frequency and the minimum of the axial ratio to lower frequency and vice versa.

Figure 10(a) and 10(b) show the effect of varying parameters of the substrate. The height h of the substrate influences the operating frequency and the shift of the minimum of the axial ratio. Decreasing the height of the substrate h leads to the shift of the operating frequency and the minimum of the axial ratio towards higher frequencies and vice versa. Very small change of the dielectric constant ϵ_r has a very small effect on the operating frequency and axial ratio.

5. Conclusion

In this paper, a circularly polarized half-mode substrate integrated waveguide U-slot antenna operating in the X-band has been proposed. The manufactured sample of the proposed antenna achieves the impedance bandwidth of 11.9% (for $S_{11} < -10$ dB), the axial ratio bandwidth of 2.2% (for $AR < 3$ dB) and the realized gain of 6.0 dBi. The proposed antenna achieves better performance and it is smaller in comparison to other HMSIW circularly polarized antennas. The proposed antenna structure can be exploited e.g. as a basic element of an antenna array for satellite communication, or for energy harvesting applications or body-centric wireless communications (after the antenna redesign for a desired frequency band).

Acknowledgment

The research described in this paper was financed by the Czech Ministry of Education in frame of the National Sustainability Program under grant LO1401. For research, infrastructure of the SIX Center was used.

References

- [1] LUO, G. Q., SUN, L. L., DONG, L. X. Single probe fed cavity backed circularly polarized antenna. *Microwave and Optical Technology Letters*, 2008, vol. 50, no. 11, p. 2996–2998. DOI: 10.1002/mop.23848
- [2] LUO, G. Q., HU, Z. F., LIANG Y., et al. Development of low profile cavity backed crossed slot antennas for planar integration. *IEEE Transactions on Antennas and Propagation*, 2009, vol. 57, no. 10, p. 2972–2979. DOI: 10.1109/TAP.2009.2028602
- [3] LUO, G. Q., SUN, L. L. A reconfigurable cavity backed antenna for circular polarization diversity. *Microwave and Optical Technology Letters*, 2009, vol. 51, no. 6, p. 1491–1493. DOI: 10.1002/mop.24393
- [4] KIM, D., LEE, J. W., CHO, C. S., et al. X-band circular ring-slot antenna embedded in single-layered SIW for circular polarization. *Electronics Letters*, 2009, vol. 45, no. 13, p. 668–669. DOI: 10.1049/el.2009.0901
- [5] KIM, D., LEE, J. W., CHO, C. S., et al. Design of SIW cavity-backed circular-polarized antennas using two different feeding transitions. *IEEE Transactions on Antennas and Propagation*, 2011, vol. 59, no. 4, p. 1398–1403. DOI: 10.1109/TAP.2011.2109675
- [6] LACIK, J. Circularly polarized SIW square ring-slot antenna for X-band applications. *Microwave and Optical Technology Letters*, 2012, vol. 54, no. 11, p. 2590–2594. DOI: 10.1002/mop.27113
- [7] XU, F., WU, K. Guided-wave and leakage characteristics of substrate integrated waveguide. *IEEE Transactions on Microwave Theory and Techniques*, 2005, vol. 53, no. 1, p. 66–73. DOI: 10.1109/TMTT.2004.839303
- [8] LAI, Q., FUMEAUX, C., HONG, W., et al. Characterization of the propagation properties of the half-mode substrate integrated waveguide. *IEEE Transactions on Microwave Theory and Techniques*, 2009, vol. 57, no. 8, p. 1996–2004. DOI: 10.1109/TMTT.2009.2025429
- [9] RAZAVI, S. A., NESHATI, M. H. Development of a low-profile circularly polarized cavity-backed antenna using HMSIW technique. *IEEE Transactions on Antennas and Propagation*, 2013, vol. 61, no. 3, p. 1041–1047. DOI: 10.1109/TAP.2012.2227104
- [10] DASHTI, H., NESHATI, M. H. Development of low-profile patch and semi-circular SIW cavity hybrid antennas. *IEEE Transactions on Antennas and Propagation*, 2014, vol. 62, no. 9, p. 4481–4488. DOI: 10.1109/TAP.2014.2334708
- [11] LAI, Q., FUMEAUX, C., HONG, W., et al. 60 GHz aperture-coupled dielectric resonator antennas fed by a half-mode substrate integrated waveguide. *IEEE Transactions on Antennas and Propagation*, 2010, vol. 58, no. 6, p. 1856–1864. DOI: 10.1109/TAP.2010.2046852
- [12] SAGHATI, A. P., MIRSALEHI, M. M., NESHATI, M. H. A HMSIW circularly polarized leaky-wave antenna with backward, broadside, and forward radiation. *IEEE Antennas and Wireless Propagation Letters*, vol. 13, no. 4, p. 451–454. DOI: 10.1109/LAWP.2014.2309557
- [13] HUBKA, P., LACIK, J. Linearly polarized HMSIW U-slot antenna. In *Proceedings of the Conference on Microwave*

Techniques (COMITE). Pardubice (Czech Republic), 2015, DOI: 10.1109/COMITE.2015.7120225

About the Authors ...

Patrik HUBKA was born in Čeladná, Czech Republic, in 1987. He received his M.Sc. degree in Electrical Engineering from Brno University of Technology (BUT), Czech Republic, in 2012, and is currently working toward the Ph.D. degree in Electrical Engineering at the Dept. of Ra-

dio Electronics, Faculty of Electrical Engineering and Communication, BUT. His research interests include microwave circuits based on HMSIW.

Jaroslav LÁČÍK received the M.Sc. and Ph.D. degrees from BUT, Czech Republic, in 2002 and 2007, respectively. He is currently an Associate Professor at the Dept. of Radio Electronics, Faculty of Electrical Engineering and Communication, BUT. His research interests are antennas, body-centric wireless communication, and computational electromagnetics. He is a member of IEEE.